AD-A169 456 DEGENERACY IN THE ENSEMBLE MONTE CARLO METHOD FOR HIGH FIELD TRANSPORT IN..(U) ARIZONA STATE UNIV TEMPE CENTER FOR SOLID STATE ELECTRONICS R.. P LUGLI ET AL. 1/1

UNCLASSIFIED 01 JUL 86 N86.3 N0014-84-K-0053 F/G 20/12 NL

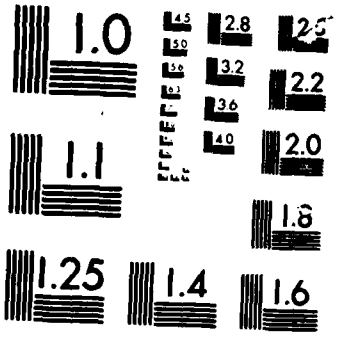

MICROCOPY CHART

(12)

UNCLASSIFIED

SECURITY CLASSIFICATION OF THIS PAGE (When Data Entered)

REPORT DOCUMENTATION PAGE		READ INSTRUCTIONS BEFORE COMPLETING FORM
1. REPORT NUMBER: N86.3	2. GOVT ACCESSION NO.: N/A	3. RECIPIENT'S CATALOG NUMBER: N/A
4. TITLE (and Subtitle): DEGENERACY IN THE ENSEMBLE MONTE CARLO METHOD FOR HIGH FIELD TRANSPORT IN SEMICONDUCTORS		5. TYPE OF REPORT & PERIOD COVERED: TECHNICAL 6. PERFORMING ORG. REPORT NUMBER
7. AUTHOR(s): P. LUGLI AND D. K. FERRY		8. CONTRACT OR GRANT NUMBER(s): N00014-84-K-0053
9. PERFORMING ORGANIZATION NAME AND ADDRESS: CENTER FOR SOLID STATE ELECTRONICS RESEARCH ARIZONA STATE UNIVERSITY TEMPE, AZ. 85287		10. PROGRAM ELEMENT, PROJECT, TASK AREA & WORK UNIT NUMBERS: RR 021-03-01 NR 619-003
11. CONTROLLING OFFICE NAME AND ADDRESS: OFFICE OF NAVAL RESEARCH (414) 800 NORTH QUINCY ARLINGTON, VA. 22217		12. REPORT DATE: 1 JULY 1986 13. NUMBER OF PAGES: 7
14. MONITORING AGENCY NAME & ADDRESS (if different from Controlling Office)		15. SECURITY CLASS. (of this report): Unclassified 15a. DECLASSIFICATION/DOWNGRADING SCHEDULE
16. DISTRIBUTION STATEMENT (of this Report): distribution unlimited		
17. DISTRIBUTION STATEMENT (of the abstract entered in Block 20, if different from Report): NA		
18. SUPPLEMENTARY NOTES		
19. KEY WORDS (Continue on reverse side if necessary and identify by block number): SEMICONDUCTORS, TRANSPORT, SCATTERING, HIGH FIELDS,		

20. ABSTRACT (Continue on reverse side if necessary and identify by block number)
An algorithm to include the Pauli exclusion principle in the Ensemble Monte Carlo method is presented. The results indicate that significant changes in the transport properties of GaAs have to be expected when degenerate conditions are reached. Important repercussions should be found in the modeling of microwave devices, where one often deals with highly doped regions.

DD FORM 1 JAN 73 1473 EDITION OF 1 NOV 65 IS OBSOLETE

SECURITY CLASSIFICATION OF THIS PAGE (When Data Entered)

Degeneracy in the Ensemble Monte Carlo Method for High-Field Transport in Semiconductors

P. LUGLI AND D. K. FERRY, SENIOR MEMBER, IEEE

Abstract—**An algorithm to include the Pauli exclusion principle in the Ensemble Monte Carlo method is presented. The results indicate that significant changes in the transport properties of GaAs have to be expected when degenerate conditions are reached. Important repercussions should be found in the modeling of microwave devices, where one often deals with highly doped regions.**

I. INTRODUCTION

THE ENSEMBLE MONTE CARLO (EMC) method has been widely used, in recent years, in connection with the study of nonlinear transport in semiconductors [1], [2]. It has also been successfully applied to the simulation of semiconductor devices [3], [4]. The EMC method is a semiclassical technique, in that it simulates electrons as classical particles undergoing scattering events that are calculated according to quantum mechanical transition probabilities. Classical statistics are used, and the Pauli exclusion principle is neglected. On the other hand, many of the situations of interest (for example, in microwave devices) involve high concentrations of electrons and impurities, where degeneracy is expected to play an important role. In the following, we propose an algorithm to include the Pauli exclusion principle in the EMC technique. Its effect on the transport characteristics of GaAs will be discussed. While attempts have previously been made to include degeneracy in a single-particle Monte Carlo, these have had only limited application [5]. Here, we show that the unique properties of the EMC allow a straightforward inclusion of degeneracy.

The influence of the exclusion principle on the average transport properties of semiconductors can be of great importance. For example, when modeling of microwave devices is treated, one often deals with highly doped regions that are expected to be degenerate. No Monte Carlo simulation of actual semiconductor devices performed so far has taken the Pauli principle into account even for concentrations well above 10^{17} cm^{-3} [6]. Furthermore, when balance equations are used [7], it is always assumed that electrons in the low field regions (typically characterized by high doping levels) have the same average kinetic energy as the lattice, in terms of their characteristic temperature. The results of the degenerate EMC calculations indicate that a proper account of the fermion statistics causes significant changes, especially to the electron "temperature" (the average energy of the carriers is related now to E_f, and not to k_BT).

Although the EMC is a semiclassical technique that simulates electrons moving as classical particles, in reality the electrons behave like fermions. They must still obey the Pauli exclusion principle: each quantum number is available for at most two electrons, which differ in their spin quantum number. Following the simple theory of the Fermi gas [8], the number of available $\vec{k}$-space states for a system enclosed in a volume V is given by $V/(2\pi)^3$. At zero temperature, the electrons fill up a region of $\vec{k}$-space called the Fermi sphere. The radius of this sphere, the Fermi wave-vector $\vec{k}_F$, is related to the electron cencentration n (at absolute zero) by

$$|\vec{k}_f| = (3\pi^2 n)^{1/3} \tag{1}$$

where n is the net electron concentration. At nonzero temperatures, electrons spill out of the Fermi sphere, moving into states previously vacant and thereby allowing for current flow to occur. In metals, only the electrons in a region of the order of k_BT_o (where T_o is the ambient temperature) from the Fermi level can take part in collision and conduction processes. Similar effects happen in semiconductors under degenerate conditions, e.g., when the Fermi level lies in the conduction band. In GaAs at 300 K, this occurs for $n > 4.6 \times 10^{17}$ cm^{-3}. The Pauli exclusion principle can be thought of as a many-body effect that influences the transport properties of degenerate semiconductors by limiting the phase space available for electronic transitions.

II. APPROACH

The probability of an electronic transition from a state $\vec{k}$ into a state $\vec{k}'$ is in general proportional to the probability $f(\vec{k})$ that the initial state is occupied and the probability $[1 - f(\vec{k}')]$ that the final state is unoccupied. Thus, the scattering rate from $\vec{k}$ to $\vec{k}'$ is then $P(\vec{k}, \vec{k}') = S(\vec{k}, \vec{k}')f(\vec{k})\,[1 - f(\vec{k}')]$, where $S(\vec{k}, \vec{k}')$ is the transition probability, usually calculated from the Fermi Golden Rule. The standard Monte Carlo procedure works within the approximation $f(\vec{k}') = 0$. That is, it considers all final states as being available. The latter method is only appli-

Manuscript received March 14, 1985; revised May 29, 1985. This work was supported in part under a grant from the Office of Naval Research.

P. Lugli is with the Dipartimento di Fisica, Universita' di Modena, 41100 Modena, Italy.

D. K. Ferry is with the Center for Solid State Electronics Research, Arizona State University, Tempe, AZ 85287.

0018-9383/85/1100-2431$01.00

cable to nondegenerate conditions, where the effect of the Pauli principle is negligible. The problem of working with $P(\vec{k}, \vec{k}')$ in the Monte Carlo algorithm lies in the fact that $f(\vec{k}')$ is not known *a priori*. However, with the EMC technique, the distribution function evolves with the ensemble and is known at every instant of time. One possibility that allows us to overcome the problem posed by the factor $[1 - f(\vec{k}')]$ is to use the differential scattering rates rather than the integrated rates in the simulation [1]. $P(\vec{k}, \vec{k}')$ can then be calculated for discrete values of the initial and final momentum and updated at fixed time intervals during the simulation. Storage requirements, however, will cause a severe limitation of the efficacy of this approach, and this suggests a different approach.

An alternative method makes use of the procedure suggested for a one-particle Monte Carlo [5]. To the best of our knowledge, this early work has been the only attempt to include the Pauli exclusion principle in Monte Carlo calculation, and has not become used since the early report. This method is extended here to the EMC technique, where it reaches real applicability. The self-consistent algorithm proposed by Bosi and Jacoboni resorts to the rejection technique [9] to account for the occupation probability of the final state at each scattering event. At the time of the selection of the particular scattering process, the final state of the transition is still not known. The exclusion principle can therefore be neglected for the determination of the length of the free flight, and for the choice of the scattering mechanism and the appropriate final state. However, once the final state is selected, $f(\vec{k}')$ is known from the EMC even during the transient phase and a random number between 0 and 1 can be used to accept or reject the transition. As the procedure is iterated, a steady state will eventually be reached, with the probability of transitions into the state $\vec{k}'$ proportional to the occupancy of that state. In principle, the distribution function is known already with the EMC and could be incorporated into the scattering rates, as suggested above. However, the continuing need to recalculate the scattering rates with this latter approach makes the rejection technique a much more efficient numerical technique.

The most delicate point of this method involves the normalization of the distribution function $f(\vec{k})$. Therefore, the extension of the method to the EMC algorithm will be described in some detail. We take N to be the number of electrons simulated in the ensemble and n the real electron concentration. Then the effective volume V of "real space" that is effectively occupied by this N-particle system is $V = N/n$. The density of allowed wave-vectors of one spin in $\vec{k}$-space is given by $V/(2\pi)^3$. A grid is set up in the three-dimensional wave-vector space, with an elementary cell whose volume is $\Omega_c = \Delta k_x \Delta k_y \Delta k_z$. Every cell can accomodate at most N_c electrons, with $N_c = 2\Omega_c V/8\pi^3$, where the factor of 2 accounts for the electron spin. For example, if we take $n = 10^{17}$ cm^{-3}, $N = 10^4$, and $\Delta k_x = \Delta k_y = \Delta k_z = 2 \times 10^5$ cm^{-1} ($k_F = 2.43 \times 10^6$ cm^{-1} at 77 K), we would have $V = 10^{-13}$ cm^3 and $N_c = 6.45$. N_c constitutes the maximum occupancy of a cell in the momentum space grid. A distribution function is defined over the grid in momentum space by counting the number of electrons in each cell. The distribution function so defined is normalized to unity by dividing the number in each cell by N_c for use in the rejection technique. We note that N_c must be sufficiently large that the roundoff to an integer does not create a significant statistical error. In the calculations discussed below, we used $\Delta k_z = 8 \times 10^4$ cm^{-1} and $\Delta k_x = \Delta k_y = 8 \times 10^5$, which assured that N_c was greater than 8. Values of N larger than 10^4 were tried to check the convergence, and no significant differences were found.

When a scattering event occurs in the EMC simulation, the cell c, containing the final state for the selected transition, is found. The normalized distribution function f_c, corresponding to that cell, is compared with a number r randomly chosen between 0 and 1. If $r > f_c$, the transition is accepted and the occupancy of cell c is increased by one. If, instead, $r < f_c$, the scattering event is treated as an additional self-scattering; it does not change the electron wave-vector. This corresponds to the introduction of an auxiliary self-scattering mechanism with probability proportional to $[1 - f(\vec{k}')]$. This rejection procedure must be included since this latter factor was ignored in the earlier steps of the EMC algorithm. In practice, however, one should keep the cell filling factors in use with the latter factor in calculating the scattering rates, but the results should be statistically the same.

The relation between real space volume, electron concentration, and the number of simulated electrons guarantees the correct normalization for the process. This selection procedure is repeated for each scattering event. The macroscopic distribution function, that is, the occupation of each cell of the grid, is updated at regular intervals (normally of the order of the typical collision time), and the procedure is iterated until the stationary distribution is obtained. As is always the case for an EMC simulation, the algorithm just described allows the analysis of the transient evolution of any given initial distribution to the steady-state one.

In the next section, the effect of the Pauli principle on the EMC results will be investigated. Furthermore, the influence of temperature, electron and impurity concentrations, and electric field on the transport properties of degenerate GaAs will be analyzed. The ensemble is composed of 10^4 electrons and only the steady-state condition will be dealt with. All of the results will be for EMC simulations of GaAs, using the two-valley model described elsewhere [10]. The fields used are sufficiently low that there is no transfer to the third set of valleys. The L-valleys are retained, however, because there is a slight possibility that the electron–electron interaction can kick some electrons to a sufficiently high energy that they will see these valleys [10]. The figures below, however, show that these electrons are very few in number and that there is no significant electron density above an energy of 0.1 eV, which is well below the threshold for transfer to the L-valleys.

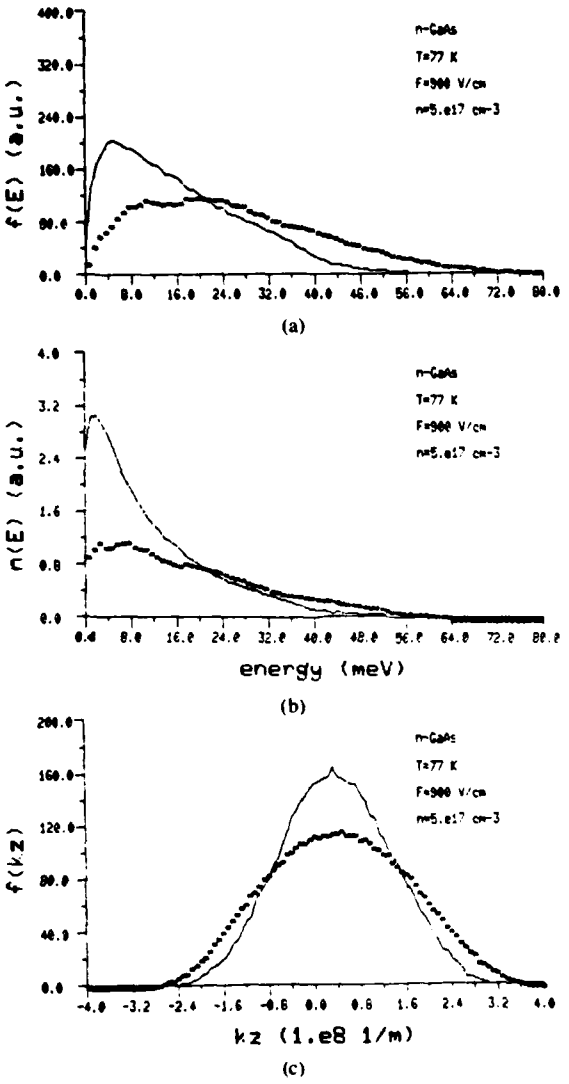

Fig. 1. (a) Energy distribution function, (b) energy occupation number, and (c) momentum distribution function, for n-GaAs, with (starred curve) and without (solid curve) the Pauli exclusion principle. The electric field is 900 V/cm, at $T = 77$ K. The electron (and impurity) concentration is 5×10^{17} cm^{-3}.

III. Results

Fig. 1 shows the effect of the exclusion principle on the electron dynamics. The continuous curves refer to the classical case; that is, they are obtained with the standard EMC simulation. The starred curves indicate the results of the inclusion of degeneracy in the manner described in the previous section. An electric field of 900 V/cm, along the z-axis, is used. The lattice temperature is 77 K, and the electron and impurity concentrations are taken to be equal to 5×10^{17} cm^{-3}.

The energy distribution function $f(E)$ in Fig. 1(a) is the number of electrons in an energy interval ΔE centered at energy E. The distribution functions here are normalized to yield the integrated value n, i.e., they give the same weighted density at E and are plotted in arbitrary units. This integration and normalization allows one very clearly to examine the shifts of particles by the changes in height (or area) at an energy value (the vertical axis is arbitrary units—a.u.). The occupation number $n(E)$ is shown in Fig. 1(b); this is obtained by normalizing $f(E)$ with respect to the number of allowed states in the corresponding energy cell, and relates more closely to the quantity f_c determined in the previous section although we are plotting the results here as a function of energy rather than momentum. The momentum distribution function $f(k_z)$, for the component of the electron momentum parallel to the field, is the projection of $f(\vec{k})$ onto the z-axis, and is shown in Fig. 1(c). The same normalization is adopted throughout this section for the various distribution functions in order to allow comparison between different figures.

As a consequence of the reduced maximum occupancy of each allowed state, electrons are pushed into the tail of the distribution. This shift corresponds to an increase of the electron "temperature" of about 50 percent (from 140 to 210 K) when the Pauli principle is included. The electron temperature T_e (in reality the average random kinetic energy of the electron) is defined in the usual manner for Monte Carlo procedures as that part of the total kinetic energy that does not include the drift component, e.g.,

$$T_e = (\hbar^2/3k_B m)\,[k_x^2 + k_y^2 + (k_z - \langle k_z \rangle)^2]. \qquad (2)$$

This corresponds to a temperature only for a nondegenerate Maxwellian distribution function. In the following, all references to temperature are to the average random kinetic energy of (2), and should be so interpreted. (We retain this usage because of its widespread use in Monte Carlo procedures, but admit that this use of the word "temperature" is not an accurate descriptor. In fact, this quantity accounts for an increase of the electrochemical potential due to degeneracy plus a real-temperature effect.) The increase of the electron temperature is also reflected in the broadening of the momentum distribution $f(k_z)$ in Fig. 1(c). On the other hand, only a small reduction of the drift velocity is observed in the degenerate situation. This is due to the increased number of phonon emission events, as more electrons are pushed above the threshold for polar optical emission processes as a result of the exclusion principle.

At lower fields (90 V/cm), the effect of degeneracy is even more pronounced, as is shown in Fig. 2. The electrons have a very small drift velocity and tend to remain in the lowest portion of the conduction band, with an average temperature nearly equal to the lattice temperature (continuous curves) in the nondegenerate case. Since it is impossible to allocate more than two electrons per state, a migration of the electrons toward higher energy states occurs (starred curves) for the case of degeneracy. In the latter case, a very high number of transitions that would normally be allowed with classical statistics are instead forbidden and thus rejected due to the occupation of the final state. In the simulations illustrated in Fig. 2, the Pauli exclusion principle prevented more than 80 percent of the almost 10^7 scattering events simulated. In this latter case, the electron temperature reaches a value of 170 K, as compared with 80 K for the nondegenerate EMC. In accor-

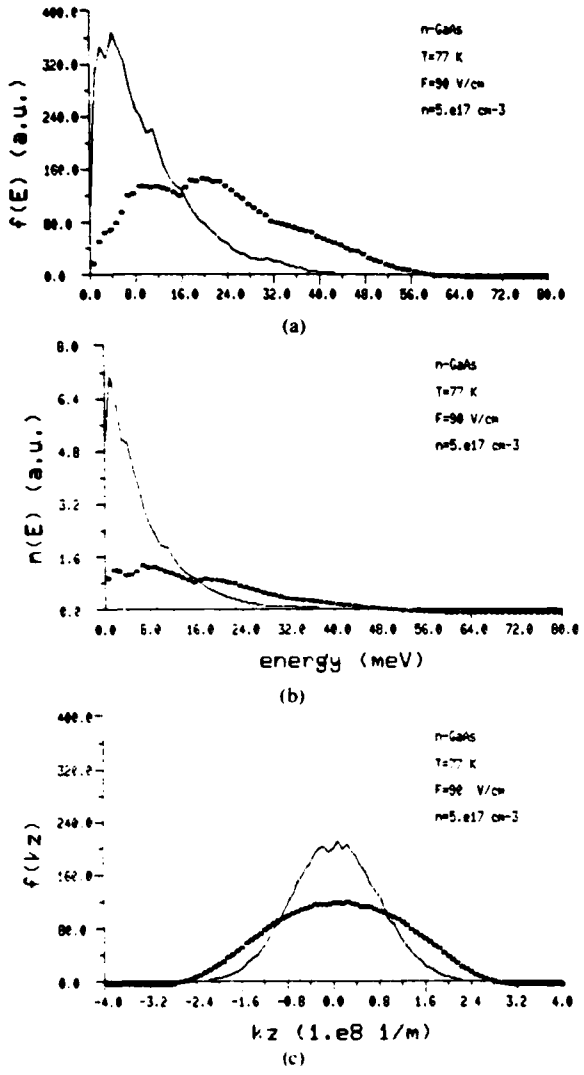

Fig. 2. (a) Energy distribution function, (b) energy occupation number, and (c) momentum distribution function, for n-GaAs, with (starred curve) and without (solid curve) the Pauli exclusion principle. The electric field is 90 V/cm, at $T = 77$ K. The electron (and impurity) concentration is 5×10^{17} cm^{-3}.

dance with the results for higher fields, the drift velocity shows only a small decrease. In Table I, we give the values of the drift velocity, average energy, and electron "temperature" for all simulations discussed in this section.

For the electric-field strengths considered in this study, impurities and polar-optical phonons constitute the major scattering processes. A simulation that keeps the same electron concentration, but greatly reduces the number of impurity centers, gives drastically different results. Fig. 3 shows the results for an impurity concentration of only 5×10^{12} cm^{-3}, while the other parameters (including the electron concentration) are left unchanged. Physically this can be achieved by exciting electrons into the conduction band of a lightly doped sample of GaAs by laser excitation, by modulation doping, or by injection over a barrier into a lightly doped region, as in a planar-doped barrier device [11]. In this situation, electrons are weakly scattered by the impurities and their drift velocity shows a

TABLE I

Non-degenerate case				Results	
n_{imp} (cm^{-3})	F (V/cm)	T_0 (K)	v_d (cm/sec)	<E> (K)	T_e (K)
$5x10^{17}$	900	77	$8.7x10^6$	139	128
$5x10^{12}$	900	77	$2.4x10^7$	190	101
$5x10^{17}$	90	77	$1.1x10^6$	81	81

Degenerate case					Results	
n_{imp} (cm^{-3})	F (V/cm)	T_0 (K)	n (cm^{-3})	v_d (cm/sec)	<E> (K)	T_e (K)
$5x10^{17}$	900	77	$5x10^{17}$	$6.1x10^6$	209	204
$5x10^{12}$	900	77	$5x10^{17}$	$2.2x10^7$	292	218
$5x10^{17}$	90	77	$5x10^{17}$	$7.5x10^6$	175	175
$5x10^{17}$	900	300	$5x10^{17}$	$4.1x10^6$	403	398
$1x10^{16}$	900	77	$1x10^{16}$	$1.5x10^7$	155	120

very sharp increase. This shift toward higher momenta is evident in Fig. 3(c), where the momentum distribution functions are compared with those for the heavily doped case (Fig. 1(c)). As a consequence of the higher drift velocity, the probability of finding electrons at high energies is also increased, as shown in Fig. 3(a) and (b). Both for degenerate and for nondegenerate statistics, the energy distribution function is broadened. The effect of the exclusion principle is reduced with respect to the heavily doped case, due to the already reduced occupancy of the low-energy states by the hotter and faster electrons.

It is interesting to note that the kink present in the continuous curve (classical case) of Fig. 3(a) at the polar-optical phonon energy (35 meV) is completely washed out in the degenerate case. This kink is the result of a strong emission of optical phonons from the streaming tail of the distribution, which creates a strong push of electrons by phonon emission back into the low-energy portion of the distribution. The streaming character of this process is also evident in the elongated tail of the momentum distribution at low momenta (continuous curve in Fig. 3(c)). The Pauli principle compensates this process by forcing the electrons back into the high-energy regions. In a way, it has exactly the same effect on the energy distribution function as the electron–electron interaction [10].

Fig. 4 isolates the effect of impurity scattering in the degenerate case. The continuous and the starred curves

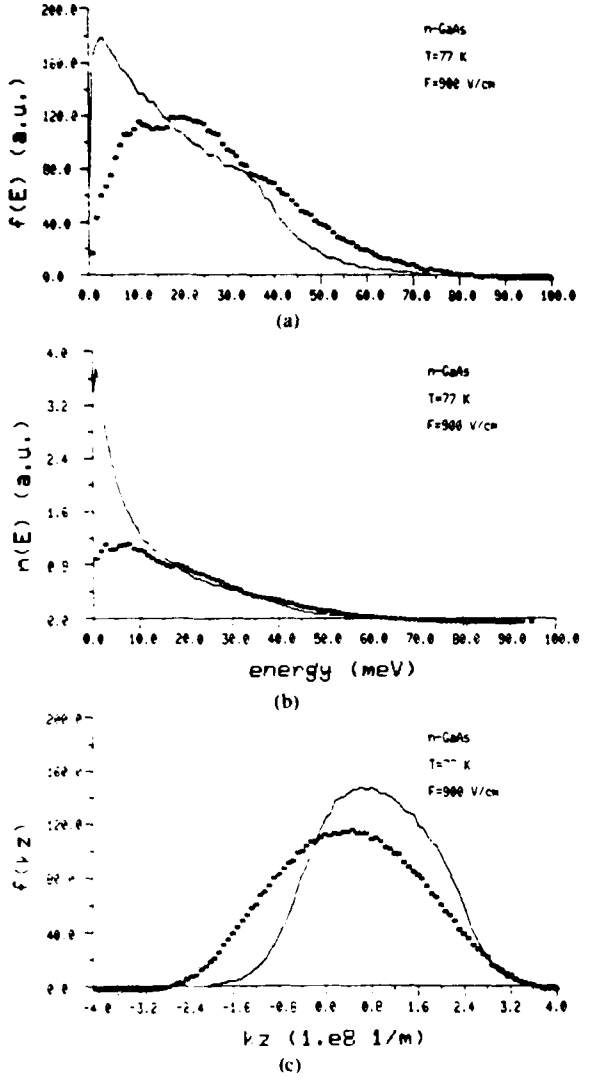

Fig. 3. (a) Energy distribution function, (b) energy occupation number, and (c) momentum distribution function, for n-GaAs, with (starred curve) and without (solid curve) the Pauli exclusion principle. The electric field is 900 V/cm, at $T = 77$ K. A low-impurity concentration is considered.

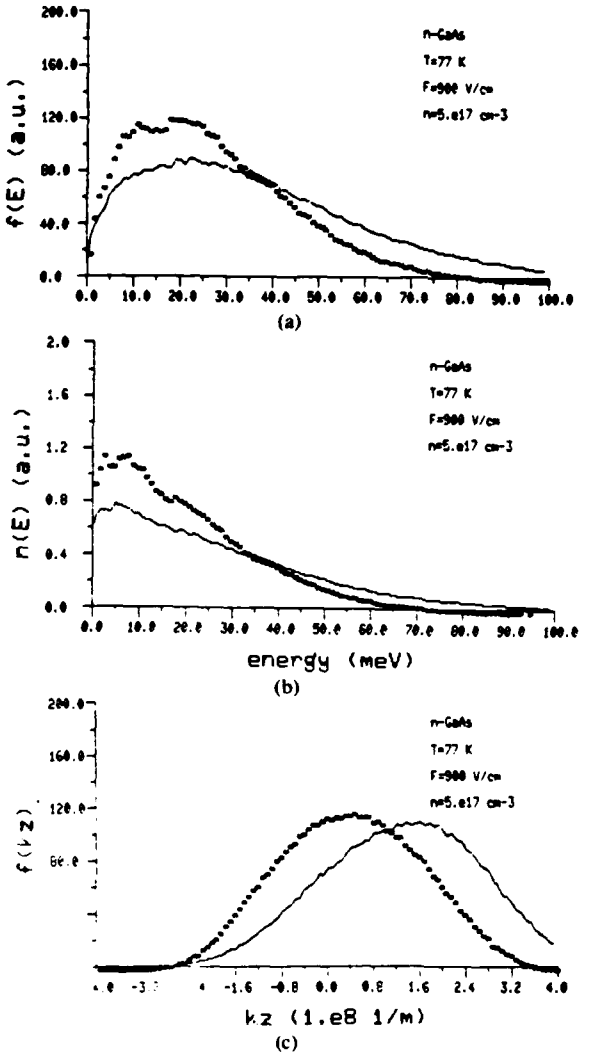

Fig. 4. (a) Energy distribution function, (b) energy occupation number, and (c) momentum distribution function, for n-GaAs, including the Pauli exclusion principle. The electric field is 900 V/cm, at $T = 77$ K. The starred curve and the solid curve are for high- and low-impurity concentration, respectively.

are for high (5×10^{17} cm^{-3}) and low (5×10^{12} cm^{-3}) concentrations, respectively. The drift velocity increases from 6×10^6 cm/s to 2.2×10^7 cm/s, as is also indicated by the shift in the momentum distribution. The increment in the drift component results in a sharp increase in the total average energy, while the electron temperature is changed only slightly (see also Table I). This velocity increase arises primarily, it is felt, from the large increase in the mobility that accompanies the decrease in doping level. This difference is significant, as it is now clear that attempts to study the electron–electron interaction by using heavily doped samples can fail due to the masking effects of the impurity scattering.

The comparison of the occupation number obtained from the present calculation and the equilibrium Fermi distribution is shown in Fig. 5. The continuous curve is for the equilibrium theoretical distribution, while the starred one is for the degenerate EMC result. The Fermi level in a

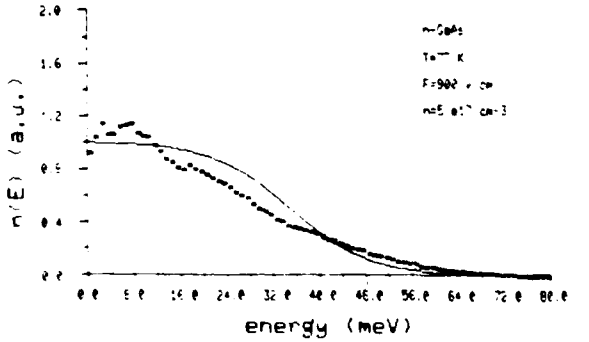

Fig. 5. Comparison of the Fermi–Dirac distribution with the EMC occupation number, for n-GaAs, at 77 K. The electron concentration is 5×10^{17} cm^{-3}, and the electric field 900 V/cm.

semiconductor at the lattic temperature T_0 is found from

$$n = n_i F_{1/2}[E_F(T_0)/k_B T_0] \tag{3}$$

where

$$n_i = 0.25(2mk_B T_0/\pi\hbar^2)^{3/2} \tag{4}$$

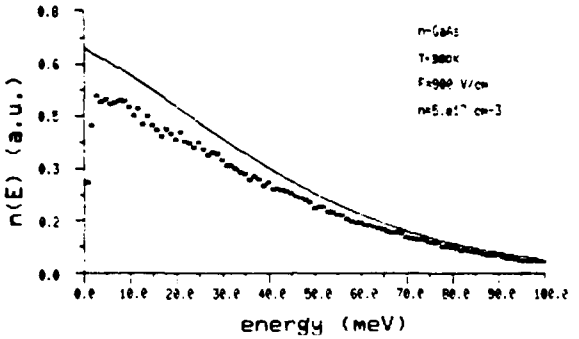

Fig. 6. Comparison of the Fermi–Dirac distribution with the EMC occupation number, for n-GaAs, at 300 K. The electron concentration is 5×10^{17} cm^{-3}, and the electric field 900 V/cm.

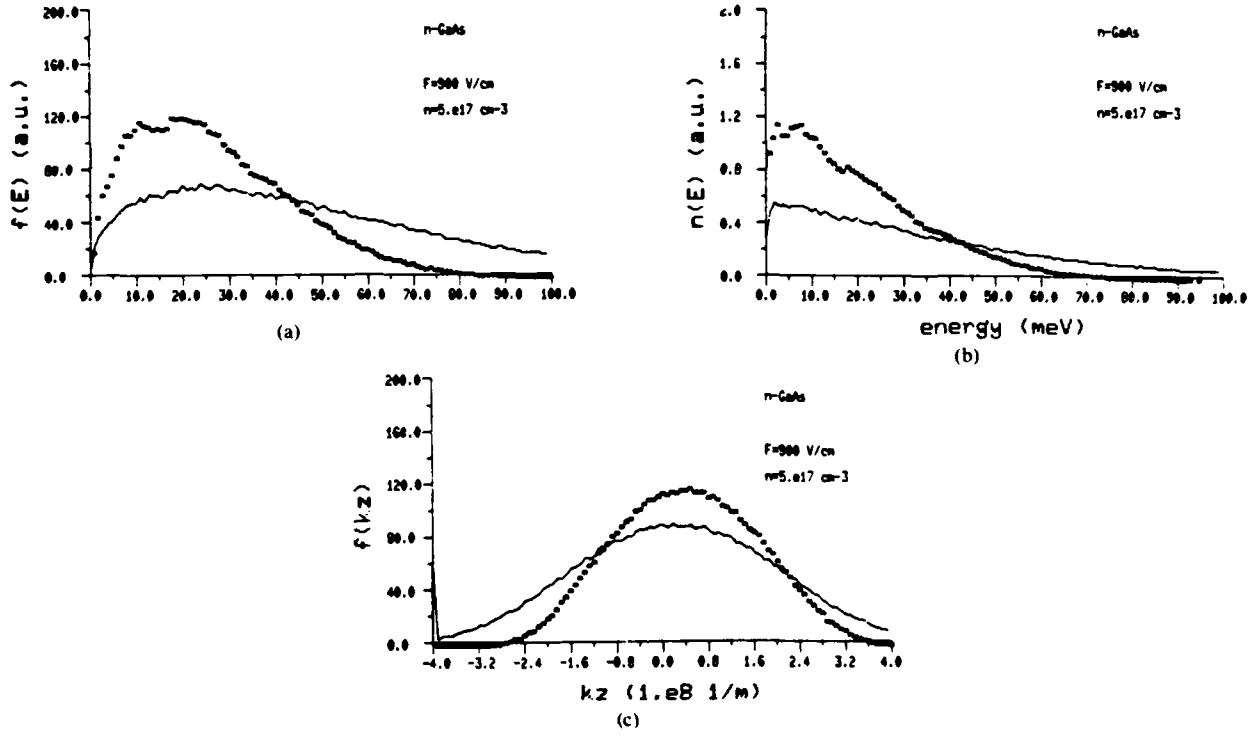

Fig. 7. (a) Energy distribution function, (b) energy occupation number, and (c) momentum distribution function, for n-GaAs, including the Pauli exclusion principle. The electric field is 900 V/cm, the electron concentration 5×10^{17} cm^{-3}. The starred curve is for $T = 300$ K; the solid one is for $T = 77$ K.

is the effective density of states in the conduction band, and $F_{1/2}$ is the Fermi–Dirac integral. In fact, the random energy given by T_e should be used in (3) and (4), and this further reduction in the Fermi energy is apparent in Fig. 5. The EMC curve is the same as shown in Fig. 1(b). At 77 K, the chemical potential is 27 meV (at $T_e = 200$ K) above the bottom of the conduction band. The noise in the lowest part of the EMC curve derives from the small number of states enclosed in the first energy cells, due to the discretization of $\vec{k}$-space described before. The higher population at high energies of the EMC curve, relative to the equilibrium curve, corresponds to the heating of the electrons, whose temperature is almost three times higher than the lattice temperature under these conditions.

At increasing ambient (or electron) temperatures, the chemical potential moves toward the bottom of the conduction band. The occupation probability of the low-energy states decreases. Fig. 6 gives the equilibrium distribution (continuous curve) and the EMC-derived distribution (starred curve) at room temperature. In this case, E_F is equal to 1.1 meV. The effect of the higher thermal motion of the electrons at room temperature is also evident by looking at the results shown in Fig. 7, where the degenerate EMC distribution function at 300 K (continuous curve) is compared with that at 77 K (starred curve).

As the electron concentration is reduced, the classical situation is approached so that the exclusion principle no

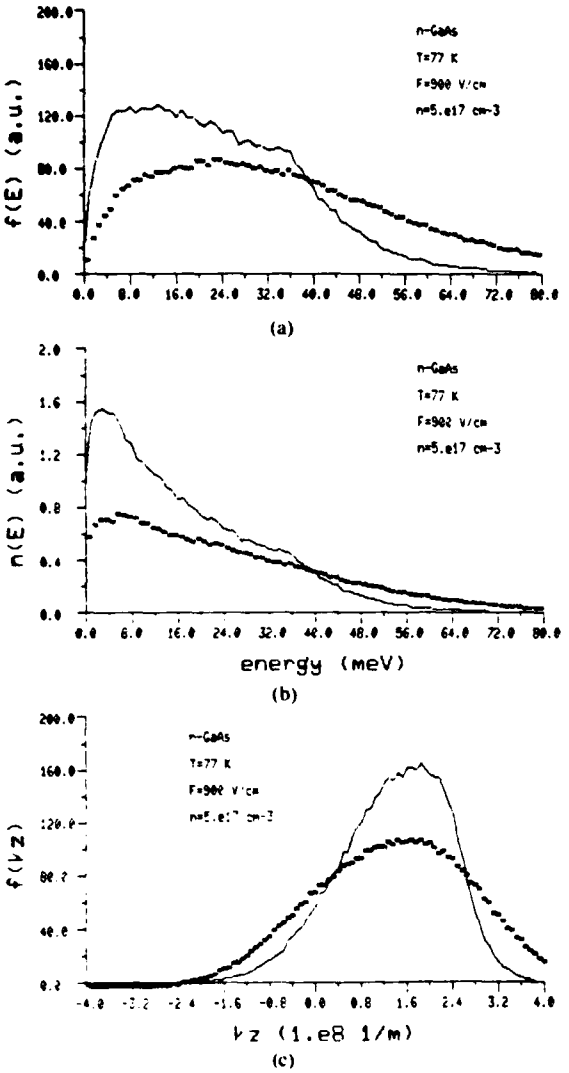

Fig. 8. (a) Energy distribution function, (b) energy occupation number, and (c) momentum distribution function, for n-GaAs, including the Pauli exclusion principle. The electric field is 900 V/cm, at $T = 77$ K. The starred curve and the solid curve are for high- and low-electron (and impurity) concentration, respectively.

longer has a significant effect. This is also a check for the consistency and correctness of the proposed method described here. Fig. 8 shows the result obtained with 10^{16} cm^{-3} electrons and impurities (continuous curve). The degenerate distributions of Fig. 1 are plotted for comparison as the starred curves. As expected, it is found that the low-density distribution coincides with the one obtained for nondegenerate statistics. No simulations have been performed at higher concentrations, since the Brooks-Herring model used to describe the interaction of the electrons with the ionized impurities breaks down and more sophisticated formulations are necessary [12].

IV. Summary

We have presented an algorithm to include the Pauli exclusion principle in an Ensemble Monte Carlo simulation through a rejection technique that utilizes the presence of an evolving EMC distribution. The results indicate that significant changes in the transport properties of GaAs have to be expected when degenerate conditions are reached. Care should be taken in device modeling where classical statistics are often used even for highly doped regions.

Acknowledgment

The authors would like to express their appreciation for helpful discussions with W. Porod and C. Jacoboni.

References

[1] P. J. Price, in *Semiconductors and Semimetals*, vol. 14, W. Willardson and A. C. Beer, Eds. New York: Academic, 1969.
[2] J. Zimmerman, P. Lugli, and D. K. Ferry, "On the physics and modeling of small semiconductor devices—IV. Generalized, retarded transport in ensemble Monte Carlo techniques," *Solid-State Electron.*, vol. 26, pp. 233-239, Mar. 1983.
[3] R. W. Hockney and J. W. Eastwood, *Computer Simulation Using Particles*. London: Wiley, 1981.
[4] E. Constant, in *The Physics of Submicron Semiconductor Devices*, H. L. Grubin, D. K. Ferry, and C. Jacoboni, Eds. New York: Plenum, in press.
[5] S. Bosi and C. Jacoboni, "Monte Carlo high-field transport in degenerate GaAs," *J. Phys. C: Solid State Phys.*, vol. 9, pp. 315-319, 1976.
[6] Y. Awano, K. Tomizawa, and N. Hashizume, "Principles of operation of short-channel gallium arsenide field-effect transistors determined by Monte Carlo method," *IEEE Trans. Electron Devices*, vol. ED-31, pp. 448-454, Apr. 1984.
[7] H. L. Grubin, in *The Physics of Submicron Semiconductor Devices*, H. L. Grubin, D. K. Ferry, and C. Jacoboni, Eds. New York: Plenum, in press.
[8] O. Madelung, *Introduction to Solid-State Physics*. Berlin: Springer, 1978.
[9] C. Jacoboni and L. Reggiani, "The Monte Carlo method for the solution of charge transport in semiconductors with applications to covalent materials," *Rev. Mod. Phys.*, vol. 55, pp. 645-705, July 1983.
[10] P. Lugli, and D. K. Ferry, "Investigation of plasmon-induced losses in quasi-ballistic transport," *IEEE Electron Device Lett.*, vol. EDL-6, pp. 25-27, 1985.
[11] R. J. Malik, T. R. Aucoin, R. L. Ross, K. Board, C. E. C. Wood, and L. F. Eastman, "Planar-doped barriers in GaAs by molecular beam epitaxy," *Electron. Lett.*, vol. ED-16, pp. 836-839, 1980.
[12] B. K. Ridley, *Quantum Processes in Semiconductors*. Oxford: Clarendon, 1982.

END

DTIC

7-86